Article

Relationship Between Soil Aggregate Stability and Associated Carbon and Nitrogen Changes Under Different Ecological Construction Measures in the Karst Region of Southwest China

Meiting Li ⓘ, Keqin Wang, Xiaoyi Ma, Mingsi Fan, Biyu Li and Yali Song *ⓘ

College of Soil and Water Conservation, Southwest Forestry University, Kunming 650224, China;
limeiting568@163.com (M.L.); wangkeqin@swfu.edu.cn (K.W.); maxiaoyi124zz@163.com (X.M.);
18388506884@163.com (M.F.); 15393876816@163.com (B.L.)
* Correspondence: songyali@swfu.edu.cn; Tel.: +86-871-3862778

Abstract: As the fundamental unit of soil structure, soil aggregates play a crucial role in enhancing soil carbon and nitrogen storage, thereby supporting soil fertility and overall health, particularly in fragile karst regions. This study aims to quantify the effects of various ecological construction measures on soil aggregate stability, including focusing on geometric mean diameter (GMD), mean weight diameter (MWD), and K values, as well as aggregate-related organic carbon (SOC) and total nitrogen (TN), soil mechanical composition, and aggregate content. The ecological construction measures examined include plantation forests (Y7th–rgl), restored forests (Y6th–zr), fruit forests (Y6th–jgl), and contour reverse slope terraces (Y1th–crt). Compared to sloping farmland, contour reverse slope terraces, with their distinctive priority induction function, significantly increased the content of medium-fine particle aggregates, greater than 87%. Among the ecological construction measures, plantation forests exhibited the highest aggregate stability, with an average increase ranging from 8% to 157%. Notably, microaggregates, regardless of size, possessed the highest carbon and nitrogen contents, contributing significantly to soil carbon and nitrogen pools. Furthermore, both plantation and contour reverse slope terrace treatments demonstrated an equal contribution of carbon and nitrogen across all aggregate sizes. The partial least squares path modeling (PLS-PM) analysis indicates that land use type and the content of carbon and nitrogen pools are the primary factors influencing soil aggregate stability. These findings suggest that plantations are particularly effective in enhancing soil and water conservation in fragile karst areas, while the contour reverse slope terrace method shows potential for stabilizing soil structure over extended time scales due to its unique "preferential entrainment" function.

Keywords: organic carbon stratification ratio; total nitrogen stratification ratio; organic carbon pool contribution; total nitrogen pool contribution; aggregate

1. Introduction

Soil aggregates are fundamental units of soil structure, formed through the binding of organic matter, clay and sand particles, polysaccharides, plant root filaments, soil mycelium, and carbonates [1]. Aggregates regulate various physical and biological processes within the soil [2,3]. During their formation and stabilization, soil aggregates play a vital role in conserving essential elements such as carbon and nitrogen, thereby improving soil fertility and enhancing structural stability [4]. Soil structural stability is critical for maintaining soil

health and productivity, especially under the influence of different ecological construction measures [5,6].

The impact of various ecological measures—such as the implementation of contour reverse-slope terraces on sloping cropland, restored forestation, fallow forest measures (plantation forestry), and the planting of fruit and economic forests—on soil aggregate stability and the associated carbon and nitrogen contents in karst landscapes has become a significant area of research. This is especially relevant for soil conservation and nutrient management [7–10]. Ecological construction measures modify ecohydrological processes by influencing vegetation cover, root structures, soil organic matter content, soil structure, and aggregate distribution, as well as surface runoff and erosion control [11–13]. However, most recent studies on different land-use types have primarily focused on soil aggregate stability and related soil properties in the Loess Plateau of China [14–18]. Although some reports exist on karst landscapes in southwest China, these studies mainly concentrate on single ecological measures and primarily examine changes in soil aggregates and organic carbon, without addressing related nitrogen content [19–21]. In particular, the effect of contour reverse-slope terraces, a key soil and water conservation measure, on soil aggregates, organic carbon, and total nitrogen (TN) content remains underreported. The varied responses of ecohydrological and soil erosion processes to different ecological construction measures can significantly alter soil depth, particle composition, vegetation cover, and other ecological dynamics, consequently influencing the content and stability of soil aggregates across different size fractions [11,15,22]. Therefore, further investigation is required to assess the effects of different ecological construction measures on soil aggregate distribution.

Soil organic matter is a complex organic compound composed of plant and animal residues, as well as products resulting from microbial transformation [23]. Organic carbon and TN are key components of organic matter, becoming immobilized in the soil through microbial activity, plant root exudates, and various physical and chemical interactions during the formation of soil aggregates. These elements are essential for maintaining soil structure and promoting fertility [23]. The composition of soil aggregates of different sizes is closely related to soil stability, carbon and nitrogen pools, and environmental quality [24–26]. Macroaggregates, in particular, are typically rich in organic carbon and nitrogen, as they tend to adsorb and stabilize organic matter more effectively, and their larger pore structures help protect these components from microbial decomposition [27]. Conversely, microaggregates, while more stable, store organic carbon and nitrogen over longer periods, but the organic matter within them is less accessible to microbes due to their smaller size and higher surface area [28,29]. Soil aggregates of varying sizes also have untapped potential for sequestering organic carbon and nitrogen, with their content generally increasing as aggregate size increases [30,31]. However, research from different regions often yields conflicting results, likely due to variations in topography, land use, soil depth, and climatic conditions [32–34]. Therefore, understanding the role of soil aggregates in carbon and nitrogen sequestration under different ecological construction measures is crucial.

Karst landscapes, characterized by their unique geological structures and complex hydrological processes, are widely distributed across various regions of the world, particularly in southern China [27,35]. The soil structure and stability in these regions are especially fragile, which leads to significant heterogeneity in soil formation processes, impacting the physical, chemical, and biological properties of the soil [36–38]. Due to the anisotropic environment, dynamic environmental factors, and the direct connectivity between surface and subsurface layers in karst regions, these areas are highly vulnerable to land degradation and pollution. This instability in the soil structure is a key contributor to the process of karst desertification [39]. Despite the widespread implementation of

soil and water conservation measures, such as contour reverse-slope terraces, alongside other ecological construction methods, their effects on SOC and nitrogen sequestration, as well as soil structural stability in karst areas, remain unclear [40,41]. In this study, we focused on five different land-use modes within the Chishui River Basin, a karst region in Yunnan, China. These modes included optimizing sloping cultivated terraces into contour reverse-slope terraces, plantation forestry measures, restored forests measures, fruit forests, and retaining sloping cultivated land as a control treatment. The primary aim was to assess the stability of soil structures under contour reverse-slope terrace measures and other ecological construction methods. We predicted that the SOC and nitrogen contents within these measures would be higher than those in the control treatment. The specific objectives of this study were (1) to evaluate the effects of different ecological construction measures on soil aggregate content and stability using the wet-sieving method, (2) to compare the changes in carbon and nitrogen contents in bulk soil and aggregates of varying sizes under different ecological construction measures in the southwest karst region, and (3) to determine the major influences affecting soil aggregate stability, erodibility, and carbon and nitrogen pools.

2. Materials and Methods

2.1. Study Area

This study was conducted in the Chishui River Basin (26°49′–28°54′ N, 104°09′–107°10′ E), which originates from Zhenxiong County, Yunnan Province, and is situated at the borders of the Yunnan, Guizhou, and Sichuan provinces. The main stream of the river spans 436.5 km, with a watershed area of 18,932.2 km^2. The basin exhibits varied topography, with higher elevations in the southwest and lower elevations in the northeast. The upper and middle reaches of the Chishui River are part of the Yunnan–Guizhou Plateau, a typical karst landscape that accounts for approximately 74% of the basin's area and is characterized by plateau mountains. The lower reaches lie in the Sichuan Basin, a Danxia landform, accounting for about 26% of the area, dominated by hilly plains. Soil types in the region include zonal yellow and yellow-brown soils, rocky limestone soils, purple soils, and cultivated paddy and dryland soils. The basin is located in the transitional zone between the plateau and the basin and experiences a continental climate, primarily in the mid-subtropical zone. Winters are dry and cold, while summers are hot and humid, with maximum temperatures reaching 39 °C, minimum temperatures dropping to −5 °C, and an average annual temperature ranging between 15 °C and 20 °C (National Meteorological Information Center, http://data.cma.cn, accessed on 15 October 2024). Annual precipitation ranges from 749 to 1286 mm, with an annual runoff of approximately 9.7 billion m^3. Rainfall is concentrated between June and September. The main crops in the region are maize and rice. Vegetation in the watershed primarily consists of plantation forests, including cedar (*Cunninghamia lanceolata*), sea buckthorn (*Hippophae rhamnoides*), firethorn (*Pyracantha fortuneana*), and osier fern (*Stenoloma fee*). Other plantation species include ash (*Fraxinus chinensis Roxb.*), Chinese crabapple (*Malus sanguinea*), and horseberry hydrangea *(Hydrangea aspera D. Don)*, as well as mugwort (*Artemisia argyi*) and *Artemisia dubia*. The location of the study area is shown in Figure 1.
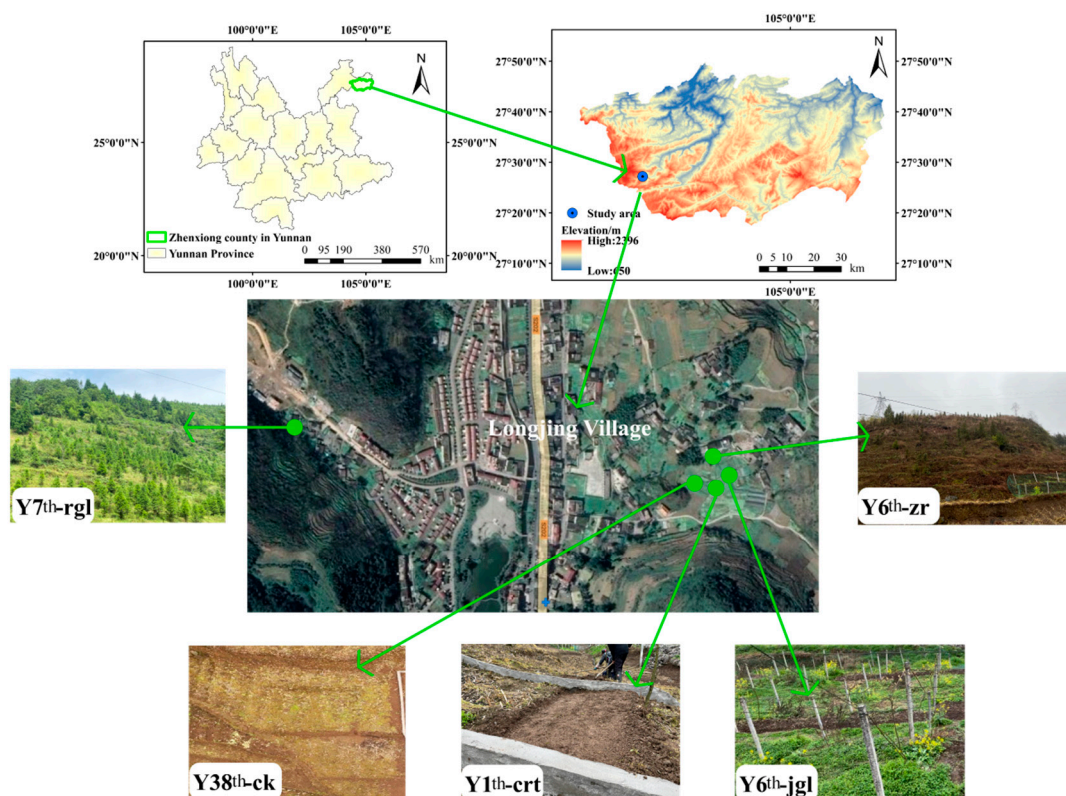
Figure 1. Location of the study area.

2.2. Sample Plot Layout and Sampling

A survey of the Chishui River Basin was conducted in 2023, with major land use types including conventional sloping cropland, plantation forests, restored forests, and fruit forests. The main rural cash crops in the basin are mainly corn, kiwifruit, etc.; however, with the economic development and the significant increase of labor price, more and more rural young and middle-aged laborers go out to work or go into business, giving up agricultural production as their main economic income and using crops such as corn for poultry rearing. Due to local production and living needs, intercropping, such as vegetables, have been added to cornfields; in addition to this, the local sloping cultivated land began to implement the terrace planting pattern in 1986 due to serious soil erosion and severe seepage from the karst landscape. However, slope farming terrace planting still leads to serious karst erosion, so the contour reverse-slope terrace measure was deployed in December 2023 to achieve the effect of runoff reduction and soil and water conservation. Natural restoration vegetation is formed with natural succession in areas with dangerous terrain and serious karst landscapes; plantation forests are formed through artificial planting and airplane dispersal. In the selection of sample plots, the years of planting were determined by visiting farmers, consulting experts, and combining with the annual cycle of vegetation succession in accordance with field research and the area covered in the field. Five construction measures were selected based on the local dominant species and planting practices: (1) Y38th–ck: Sloping cultivated terraces with 38 years of continuous cultivation, where corn was planted, served as the control treatment. (2) Y1th–crt: Considering the typical local karst geomorphology and severe soil erosion, contour reverse-slope terrace measures were implemented in sloping cropland continuously cultivated for 38 years (Figure 2). Specifically, contour terraces were constructed along the slope at intervals of 5 to 10 m, depending on the gradient, to divide the original slope into smaller segments. This reduced the length of slopes that facilitate surface runoff [37,38]. A "preferential entrainment" func-

tion formed in contour reverse-slope terrace ditches, which allowed for soil particles and organic matters to be deposited in the ditches, thereby reducing soil and nutrient erosion. (3) Y7th–rgl: Retiring measures were implemented in 2017. (4) Y6th–zr: Due to the high rock content of the karst landscape, agricultural activities were challenging. Thus, in 2018, restored forestation was initiated to prevent erosion and mitigate the decline in agricultural productivity. (5) Y6th–jgl: In 2018, the original crops (corn, peppers, etc.) were replaced with a fruit forest, and kiwifruit trees were planted in the orchard year-round.
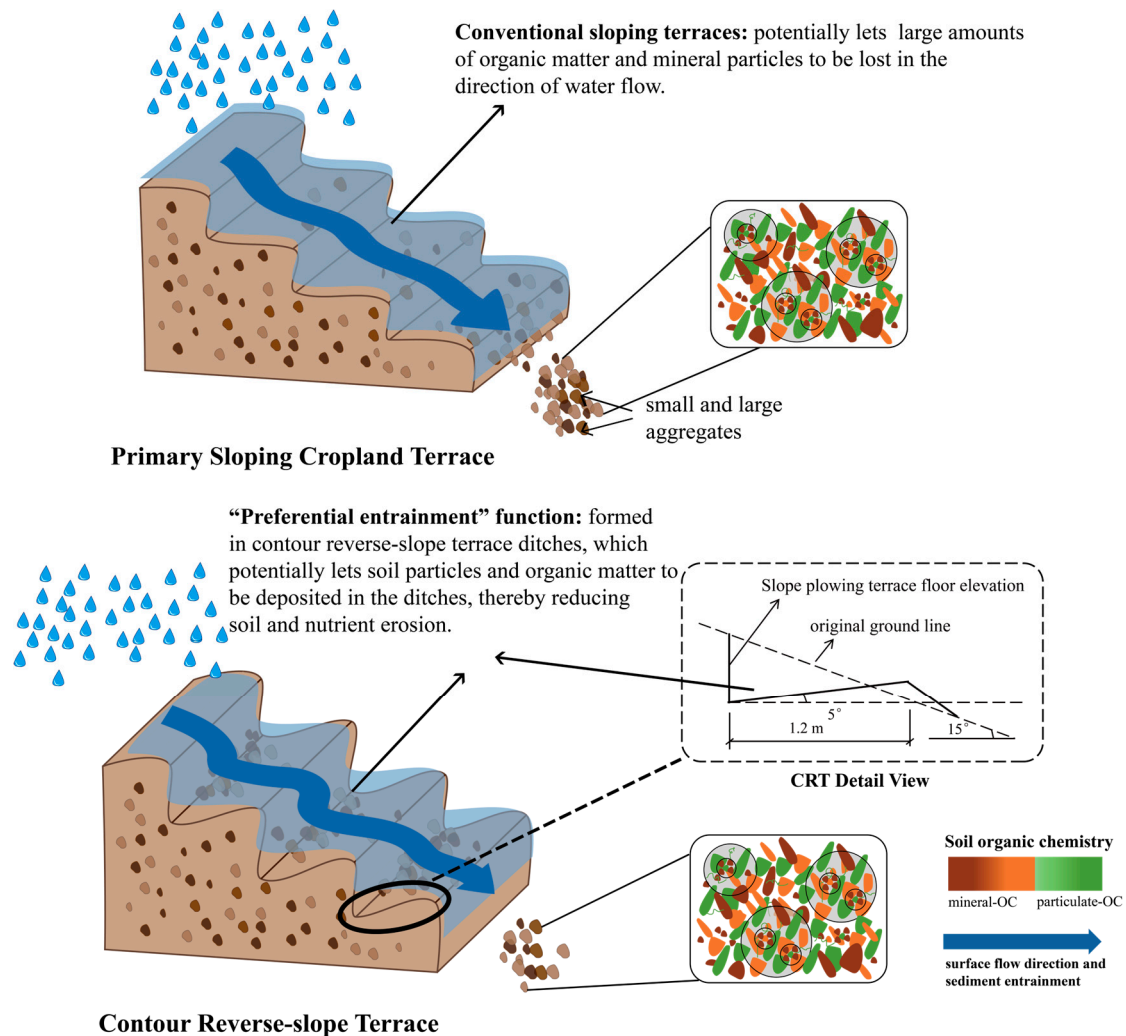

Figure 2. Schematic diagram of contour reverse-slope terrace step.

Sampling for the five ecological construction measures took place in late March 2024. Within each of the five treatments, three 1 m × 1 m plots were randomly selected as replicates. Soil samples were collected from three soil depths (0–10 cm, 10–20 cm, and 20–30 cm) in each replicated plot. Samples from the "preferential entrainment" areas of the contour reverse-slope terraces were also collected. In total, 45 soil samples were obtained for this study.

2.3. Experimental Analysis

Prior to air-drying, the collected soil samples were manually broken down into particles smaller than 5 mm. After air-drying, a portion of the samples was subjected to dry sieving to classify the soil aggregates into large aggregates (>2 mm), medium aggregates (2–0.25 mm), and microaggregates (<0.25 mm). These classified aggregates were then

used to determine the content of different soil aggregates as well as SOC and TN levels in each aggregate size. The remaining soil samples were sieved through a 0.25 mm mesh to determine the SOC and TN content in the bulk soil. SOC content was measured using the external heating method with potassium dichromate, while TN content was determined using the Kjeldahl method. The mechanical composition of the soil, including its sand, silt, and clay content, was measured using a Malvern laser particle size analyzer. The classification of soil particles was conducted according to United States standards.

To evaluate the effects of different ecological construction measures on soil aggregate stability, two key indicators—mean weight diameter (MWD) and geometric mean diameter (GMD)—were calculated based on the weights of the macro- and microaggregates and their respective mean diameters, using the following equations:

$$MWD = \sum_{i=1}^{n} X_1 M_i \tag{1}$$

$$GMD = \exp\left[\sum_{i}^{n} M_i \cdot \ln(X_i)\right] \tag{2}$$

where n represents the number of aggregate size classes (in this case, three), M_i is the weight percentage of agglomerate i relative to the total weight of the soil sample, and X_i is the average diameter of agglomerate i.

The stratification ratios (SRs) of SOC and TN, which are critical indicators for assessing the distribution of organic carbon and nitrogen at different soil depths, were also calculated. These ratios provide valuable insights into soil management, land use practices, and ecological health, aiding the development of sustainable agricultural and soil management strategies. The SRs for SOC and TN were calculated using the following equations:

$$SR_{SOC1} = SOC_{0-10}/SOC_{10-20} \tag{3}$$

$$SR_{SOC2} = SOC_{0-10}/SOC_{20-30} \tag{4}$$

$$SR_{TN1} = TN_{0-10}/TN_{10-20} \tag{5}$$

$$SR_{TN2} = TN_{0-10}/TN_{20-30} \tag{6}$$

where SOC_{0-10}, SOC_{10-20}, and SOC_{20-30} represent the SOC content at soil depths of 0–10 cm, 10–20 cm, and 20–30 cm, respectively, and TN_{0-10}, TN_{10-20}, and TN_{20-30} represent the corresponding TN content.

Differences in the mass percentages of soil aggregates of varying sizes, as well as the organic carbon and TN contents within these aggregates, result in variations in SOC and TN sequestration in the entire soil profile under different ecological construction measures. To assess the contribution of aggregates of different sizes to the total SOC and TN pools under varying ecological measures, the following equations were used:

$$C_{ai} = \frac{W_{ai} \times SOC_{ai}}{w_b \times SOC_b} \times 100\% \tag{7}$$

$$C_{ai} = \frac{W_{ai} \times TN_{ai}}{w_b \times TN_b} \times 100\% \tag{8}$$

where Wai represents the mass weight of agglomerate i; SOC_{ai} and TN_{ai} are the organic carbon and nitrogen contents of agglomerate i; W_b is the mass weight of the whole soil; SOC_b and TN_b are the total organic carbon and TN contents of the whole soil. C_{ai} denotes the contribution of agglomerate i to the SOC pools and TN pools.

The soil erodibility K value is determined using the EPIC model proposed. This model estimates the K value based on soil particle composition and the content of soil organic carbon. The calculation formula is as follows:

$$
\begin{aligned}
K_{EPIC} \;=\; & \left\{ 0.2 + 0.3\exp\left(-0.0256 \times SAN \times \left(1 - \tfrac{SIL}{100}\right)\right)\right\} \times \left(\tfrac{SIL}{CLA+SIL}\right)^{0.3} \\
& \times \left(1.0 - \tfrac{0.25 \times C}{C + \exp(3.72 - 2.95 \times C)}\right) \\
& \times \left(1.0 - \tfrac{0.7 \times \left(1 - \tfrac{SIL}{100}\right)}{\left(1 - \tfrac{SIL}{100}\right) + \exp\left(-5.52 + 22.9 \times \left(1 - \tfrac{SIL}{100}\right)\right)}\right)
\end{aligned}
\tag{9}
$$

Among them, SAN, SIL, and CLA correspond to sand content (%), powder content (%), and clay content (%), respectively; C is organic carbon content (%).

The K value calculated from the aforementioned equation is expressed in US units and must be converted to SI units (t·hm^2·h/(MJ·mm·hm^2)) by multiplying by 0.1317. The K value proposed by Zhang et al. (2008) [39] has been modified to effectively adapt to the estimation of soil erodibility in my country, as follows:

$$
K = -0.01383 + 0.515751\, K_{EPIC}
\tag{10}
$$

2.4. Statistical Analysis

In this study, we comprehensively assessed the effects of ecological construction measures, soil aggregates, soil depth, and their interactions on soil organic carbon and nitrogen content. Three-factor analysis of variance (ANOVA) was chosen because it was able to consider these three key factors and their interactions simultaneously, adapt to the data structure of the subgroup design in the study, and reveal the relative importance and interaction mechanisms of different factors. One-way ANOVA was used to test the effects of a single factor (ecological construction measures) on multiple dependent variables, to meet the need for multiple comparisons, and to accurately assess the effects of different measures, while Pearson's correlation analysis was used to explore the linear correlations between soil variables under different ecological construction measures at a significance level of $p < 0.05$, to control errors in statistical inference, and to provide a useful tool for understanding the interactions between soil carbon and nitrogen cycling and the nature of aggregates' interactions with agglomerate properties. Linear regression analysis was used to assess the relationship between different aggregates and soil carbon and nitrogen content, to establish a model to quantify the degree of influence of aggregates, and to clarify the mechanism of their role in soil carbon and nitrogen cycling. The partial least squares method comprehensively analyzes the multifaceted effects of land use type, mechanical composition, agglomerate composition, and carbon and nitrogen pools on the stability of agglomerates and extracts the main influencing factors through dimensionality reduction to simplify the process of data analysis and improve the explanatory power and predictive ability of the model. All graphs were plotted by Origin 2022 and R v 4.4.1 language, and SPSS16.0 software was used for statistical analysis.

3. Results

3.1. Change in Aggregate and Soil Texture Content

Under different ecological construction measures, macroaggregates had the highest content among the three aggregate size classes (Figure 3). Across the 0–30 cm soil depth, the average content of macroaggregates, medium aggregates, and microaggregates was 58%, 38%, and 4%, respectively. The highest macroaggregate content was observed in the Y38th–ck treatment (61%), followed by Y7th–rgl (60%), while the lowest was Y1th–crt (53%). Specifically, the macroaggregate content in Y38th–ck was 1.16 and 1.11 times higher than that of Y1th–crt and Y7th–rgl, respectively. In contrast, Y1th–crt showed the highest content

of medium aggregates (43%) and microaggregates (7%), representing increases of 1% and 1%, respectively, compared to Y6th–zr. Additionally, Y1th–crt exhibited an 86% increase in microaggregate content compared to Y38th–ck, while Y7th–rgl showed a 2% increase. However, Y6th–jgl had a 59% decrease in microaggregate content compared to Y38th–ck. In Y1th–crt, the ratio of macroaggregates to medium aggregates was approximately 1.21, and the ratio of macroaggregates to microaggregates was around 8.00. This treatment displayed a more balanced distribution of aggregate proportions, with the smallest difference between medium and microaggregate contents compared to the other four ecological construction measures.
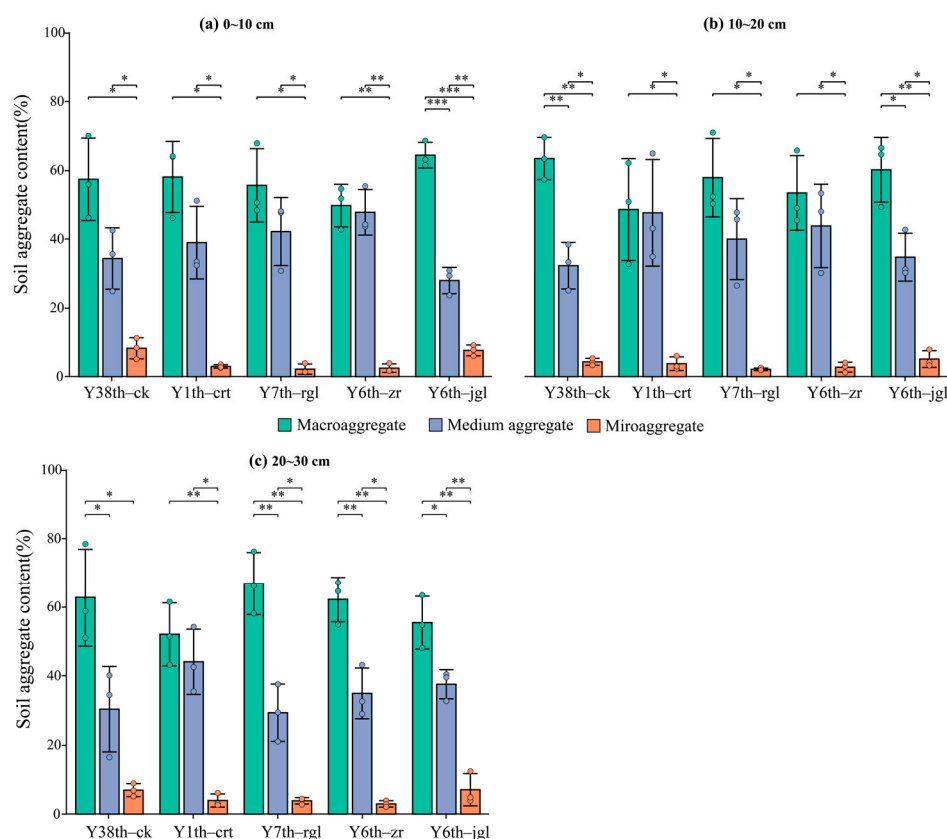

Figure 3. Changes in soil aggregate content of different treatments. * represents *p* < 0.05, ** represents *p* < 0.01, *** represents *p* < 0.001. (**a**–**c**) Respectively, soil layers 0–10 cm, 10–20 cm, and 20–30 cm. The same below.

Overall, the Y1th–crt treatment showed an increased proportion of medium and microaggregates compared to the other ecological construction measures, highlighting its potential advantages in stabilizing soil structure.

(Figure 4) Under various treatments, all except for Y1th–crt exhibited a mechanical composition characterized by the highest proportions of clay and silt (*p* < 0.05), with silt constituting 60% of the overall soil composition. The proportions of silt, clay, and sand did not show significant variation with soil depth. Among the three soil layers, the clay content in the Y6th–zr treatment was typically the highest, averaging a 7% increase compared to Y38th–ck. The silt content in the Y7th–rgl treatment was also the highest, ranging from 1.13 to 1.24 times that of Y38th–ck, while the sand content was predominantly highest in the Y1th–crt treatment.
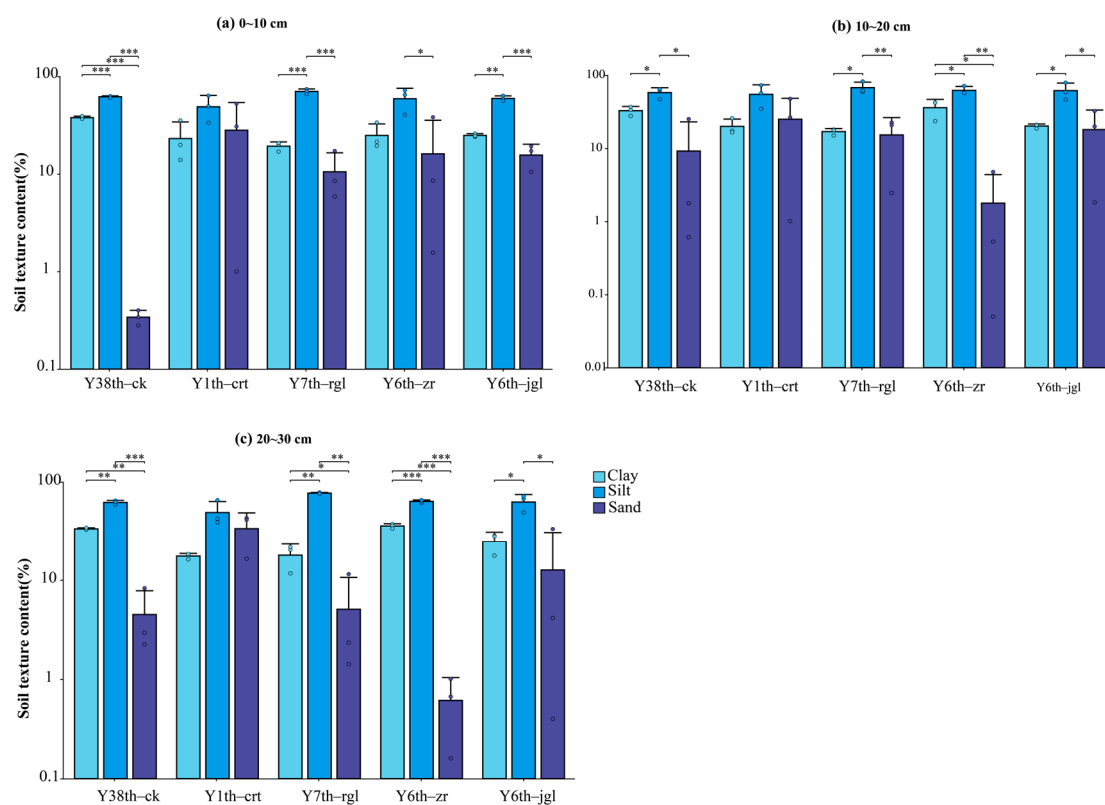
Figure 4. Soil texture content of different treatments. * indicates $p < 0.05$, ** indicates $p < 0.01$, and *** indicates $p < 0.001$.

3.2. Aggregate Stability and Erodibility

Among the three soil layers, the highest GMD values were observed in the Y7th–rgl treatment. On average, the GMD values for Y7th–rgl were 8% to 157% higher than those of the other ecological construction measures (Figure 5). In contrast, the structural stability of Y38th–ck was the lowest, with GMD values 15% to 35% lower than the other measures. In the 0–20 cm soil layer, the highest MWD value was found in the Y6th–jgl treatment, with an average value of 2.60, which was 1.06 to 1.15 times higher than the other ecological construction measures. In the 20–30 cm soil layer, the highest MWD value was recorded in Y7th–rgl (3.10), following the same trend as the GMD values. This was 10% higher than the MWD value in Y6th–jgl. Soil erodibility (Figure 5) across different soil layers was lowest in the Y1th–crt treatment, which exhibited a 36% reduction compared to the Y38th-ck treatment. The geometric mean diameter (GMD, or mean weight diameter, MWD) and K values under various treatments demonstrated the following trends: Y7th-rgl > Y6th-zr > Y6th-jgl > Y1th-crt > Y38th-ck and Y38th-ck > Y7th-rgl > Y6th-zr > Y6th-jgl > Y1th-crt.
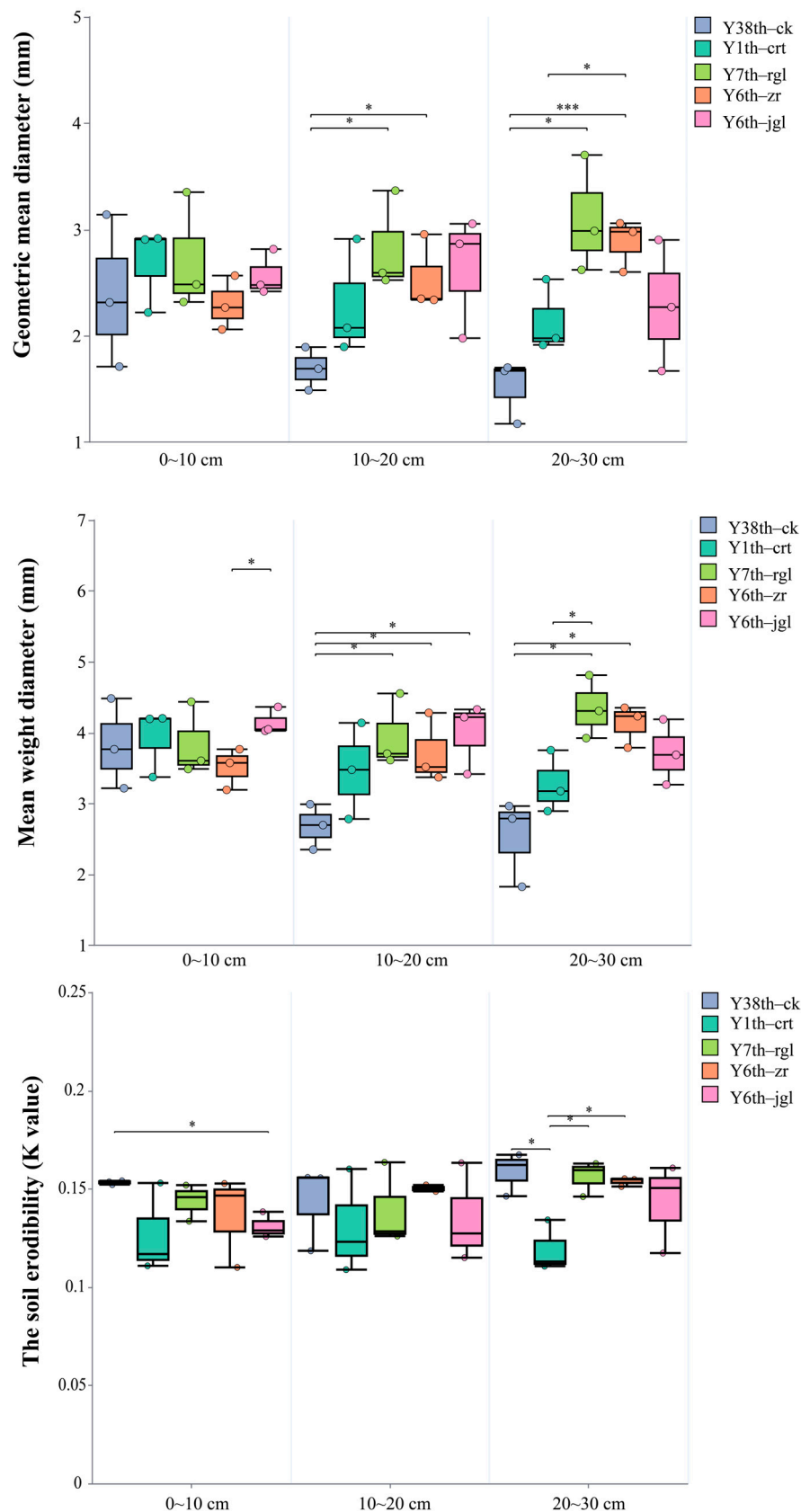
Figure 5. Stability of soil aggregates of different treatments. * indicates *p* < 0.05 and *** indicates *p* < 0.001.

3.3. Changes in Organic Carbon and TN Content in Whole Soil and Aggregates

The results of the three-factor ANOVA indicated that ecological construction measures, soil aggregates, and soil depth had significant effects ($p < 0.001$) on both total organic carbon and nitrogen content, as well as on the carbon and nitrogen content within soil aggregates (Tables 1 and 2). Overall, the average organic carbon and TN content across the five ecological construction measures decreased with increasing soil depth, with the highest values consistently found in microaggregates (Figure 6). The Y38th–ck treatment exhibited the lowest values of organic carbon and TN across all aggregate sizes and in the whole soil. Among the macroaggregates, the Y6th–zr treatment had the highest TN content (1.33 g/kg), which was 123% greater than the lowest value in Y38th–ck (0.60 g/kg). Additionally, Y6th–zr also had the highest organic carbon content (51.07 g/kg), which was 2.66 times higher than that of Y38th–ck and 28% higher than Y1th–crt. For medium aggregates, Y6th–zr also recorded the highest TN content (1.39 g/kg), 2.44 times greater than Y38th–ck (0.57 g/kg). The organic carbon content of Y7th–rgl was 53.33 g/kg, which was 2.61 times higher than Y38th–ck. Among the microaggregates, the TN content of Y6th–zr (1.32 g/kg) was significantly higher than Y38th–ck (0.60 g/kg), while Y7th–rgl had a TN content of 1.21 g/kg, representing a 102% increase over Y38th–ck. The organic carbon content in the Y6th–zr treatment was 56.51 g/kg, also 2.61 times greater than Y38th–ck. Overall, the Y6th–zr treatment performed best in terms of whole SOC and TN contents, with values of 53.08 g/kg and 1.25 g/kg, respectively. Across all three soil layers, the trends in organic carbon and TN content in both aggregates and whole soil under the five ecological construction measures followed the same pattern: Y7th-rgl > Y6th-zr (Y6th-zr > Y7th-rgl) > Y1th-crt > Y6th-jgl > Y38th-ck.

Table 1. Effects of ecological construction measures, soil layers, and aggregates on organic carbon content.

	Ecological Construction Measures (ECM)	Soil Depth (SD)	Aggregates (AG)	ECM × SD	ECM × AG	SD × AG	ECM × SD × AG
df	4	2	2	8	8	4	16
F	2149.042	297.609	75.838	12.53	6.59	13.441	5.299
p	<0.001	<0.001	<0.001	<0.001	<0.001	<0.001	<0.001

Table 2. Effects of ecological construction measures, soil layers, and aggregates on total nitrogen content.

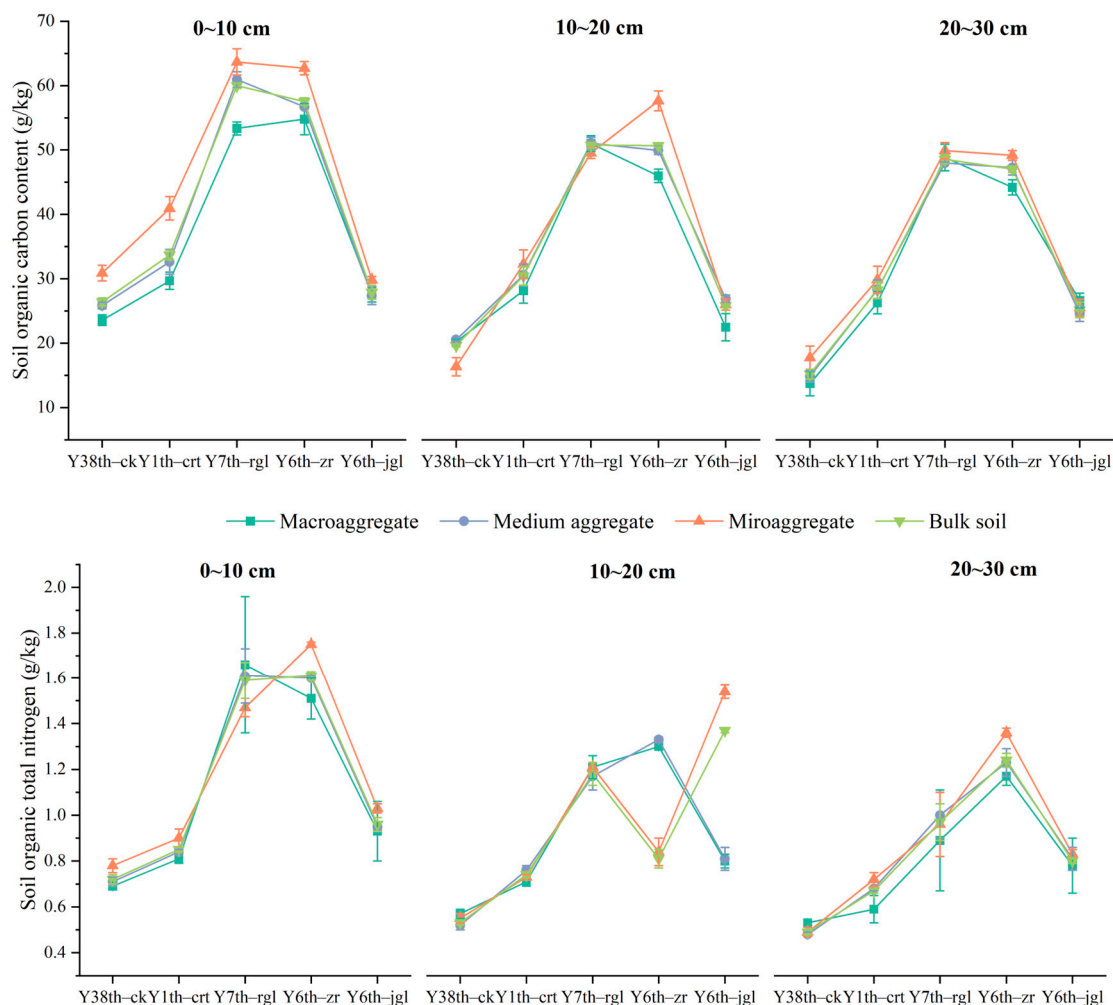|	Ecological Construction Measures (ECM)	Soil Depth (SD)	Aggregates (AG)	ECM × SD	ECM × AG	SD × AG	ECM × SD × AG
df	4	2	2	8	8	4	16
F	375.023	135.046	5.794	10.001	2.908	0.326	0.686
p	<0.001	<0.001	<0.05	<0.001	<0.05	0.86	0.801

Figure 6. Organic carbon and total nitrogen content of different treatments.

3.4. Relationship Between Organic Carbon and TN Content in Different Aggregates and Bulk Soil

Simple linear regression analysis revealed that the relationship between whole-SOC and nitrogen content and the organic carbon and nitrogen content within different aggregates was close but not statistically significant ($p > 0.05$) (Figure 7). In the 0–30 cm soil layer, the regression coefficient for organic carbon content in large aggregates (b = 0.77) was higher than that for medium aggregates (b = 0.71) and microaggregates (b = 0.66). Conversely, the regression coefficients for TN content in large aggregates (0–10 cm: b = 0.031; 10–20 cm: b = 0.029; 20–30 cm: b = 0.0339) were lower than those for medium aggregates (0–10 cm: b = 0.029; 10–20 cm: b = 0.0295; 20–30 cm: b = 0.039) and microaggregates (0–10 cm: b = 0.0339; 10–20 cm: b = 0.0332; 20–30 cm: b = 0.03442).

The Y7th–rgl treatment exhibited the highest SRs for both organic carbon and TN (SR_SOC = 1.35, 1.74; SR_TN = 1.35, 1.66), which were significantly higher than those of the other ecological construction measures (Figure 8), showing increases of 18.4% to 57% compared to the other four treatments. This increase was statistically significant. In contrast, Y38th–ck had the lowest SRs (SR$_{SOC}$ = 1.08, 1.11; SR$_{TN}$ = 1.14, 1.27), with no significant increase observed. The SRs for Y1th–crt were 1.02 to 1.12 times higher than those of Y38th–ck.
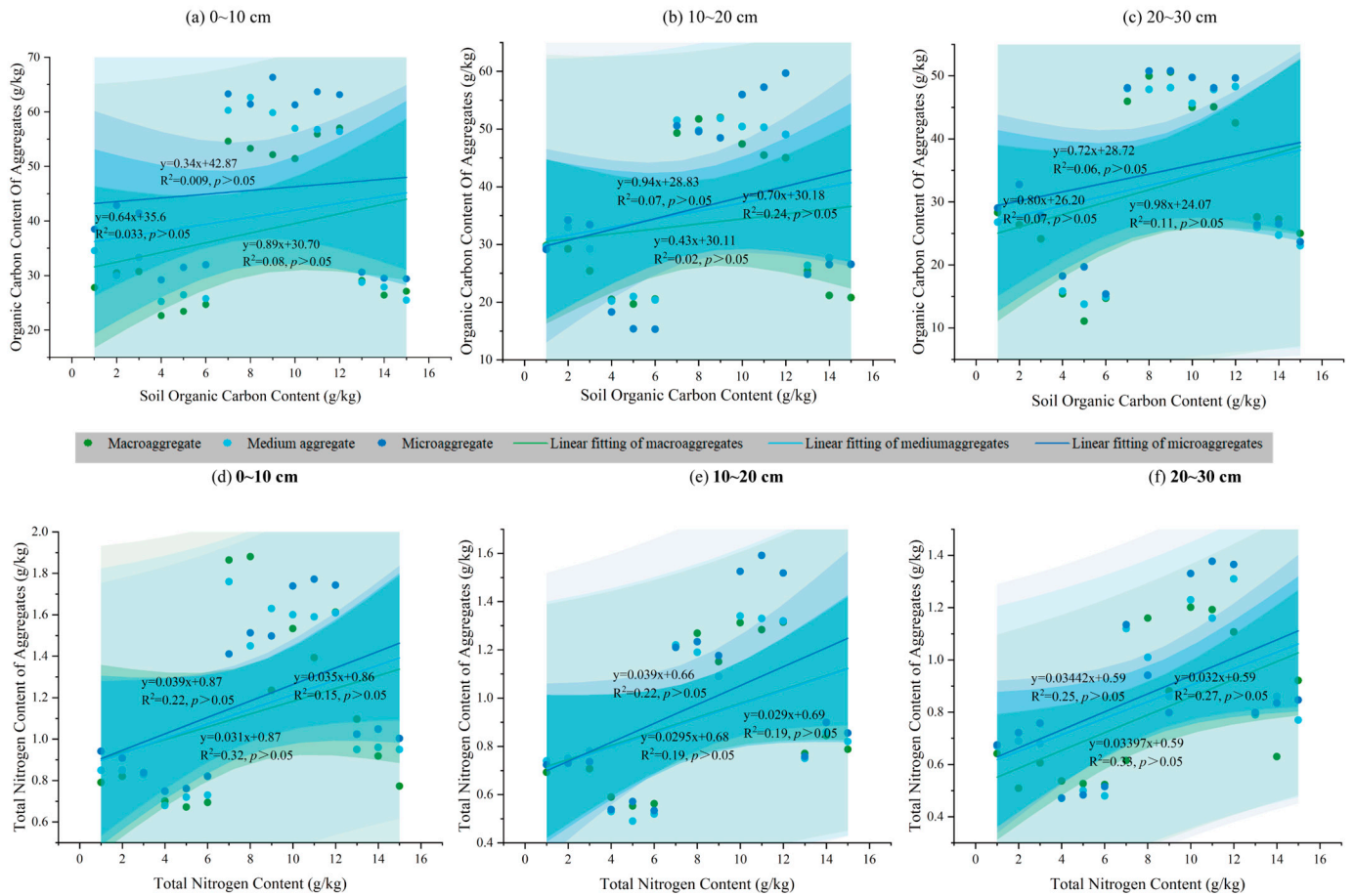
Figure 7. Linear relationship between organic carbon and total nitrogen content in different aggregates and organic carbon and total nitrogen content in different aggregates.
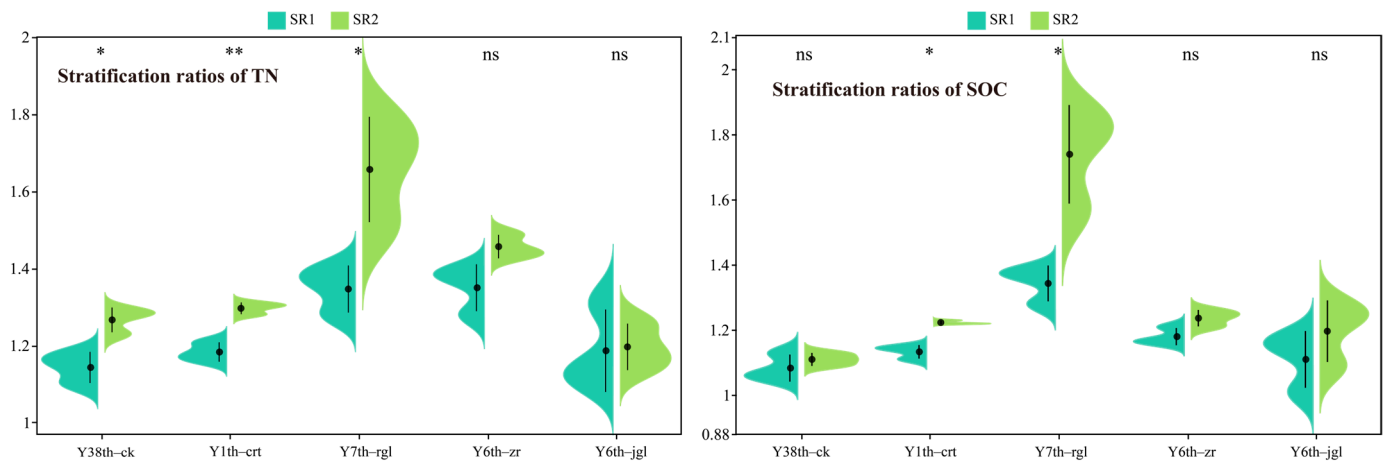

Figure 8. Stratified ratios of total organic carbon and nitrogen to organic carbon and total nitrogen content within aggregates under different ecological construction measures. ns denotes no significant difference, * denotes $p < 0.05$, ** denotes $p < 0.01$.

3.5. Contribution of Different Soil Aggregates to Organic Carbon and TN Pools

Different ecological construction measures significantly influenced the contribution of various soil aggregates to the organic carbon and TN pools (Figure 9). Across all five ecological measures, the largest contribution to both the organic carbon and TN pools came from large aggregates. As particle size decreased, the contribution of aggregates to these pools significantly declined. In the 0–30 cm soil layer, Y6th–jgl showed the highest

contribution from large aggregates to both organic carbon and TN pools. This was 1.35 to 1.49 times greater than the contributions from Y1th–crt, Y38th–ck, Y7th–rgl, and Y6th–zr ($p < 0.05$). Among medium aggregates, Y7th–rgl had the highest contribution to organic carbon and TN pools, representing a 1% to 30% increase compared to the other four ecological construction measures ($p < 0.05$). Both Y7th–rgl and Y1th–crt displayed relatively even contributions to TN pools, indicating a more balanced distribution of nitrogen within medium aggregates, which suggests potential for stabilizing nitrogen content in the soil. For microaggregates, Y6th–zr showed the highest contribution to the organic carbon pool, which was 1.02 to 2.38 times higher than that of the other treatments. Overall, the contributions of organic carbon and TN from the three types of aggregates were most consistently balanced in the Y7th–rgl and Y1th–crt treatments. These findings suggest that these two treatments may promote a more integrated and stabilized nutrient cycling process within the soil matrix.
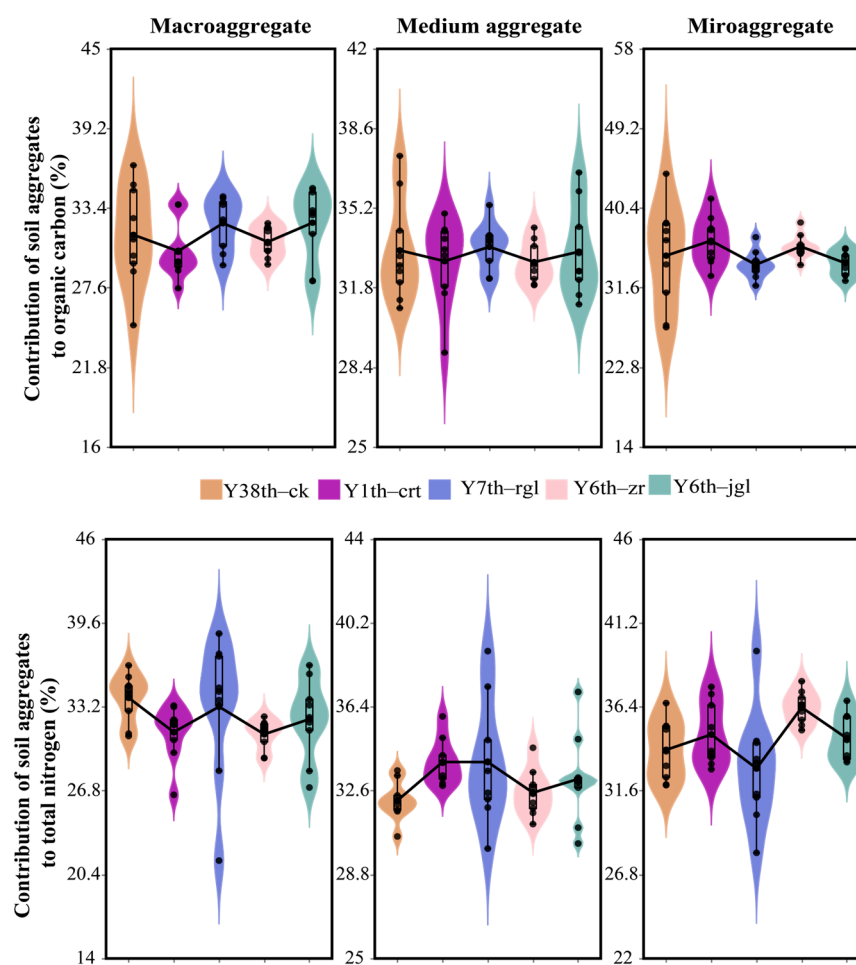

Figure 9. Contribution of different aggregates to carbon and nitrogen pools under different ecological construction measures.

3.6. Correlation of Stability with Soil Properties

A positive correlation ($p < 0.001$) was found between GMD, MWD, and K values in the 0–30 cm soil layer (Figure 10). Additionally, silt content, GMD, MWD, and K values exhibited a positive correlation ($p > 0.05$) with the content of MA, MA-SOC, MI-SOC, ME-SOC, BS-SOC, BS-TN, MA-TN, ME-TN, and MI-TN. Macroaggregate content in the soil was positively correlated with both SOC and TN contents ($p > 0.05$). In contrast, ME, MI, clay, and silt content showed a negative correlation with MWD, GMD, SOC, and TN content ($p > 0.05$), whereas MA content demonstrated a positive correlation with MWD,

GMD, K values, SOC, and TN contents ($p > 0.05$). Moreover, the organic carbon content in both the whole soil and aggregates was positively correlated with the associated TN content ($p < 0.001$).
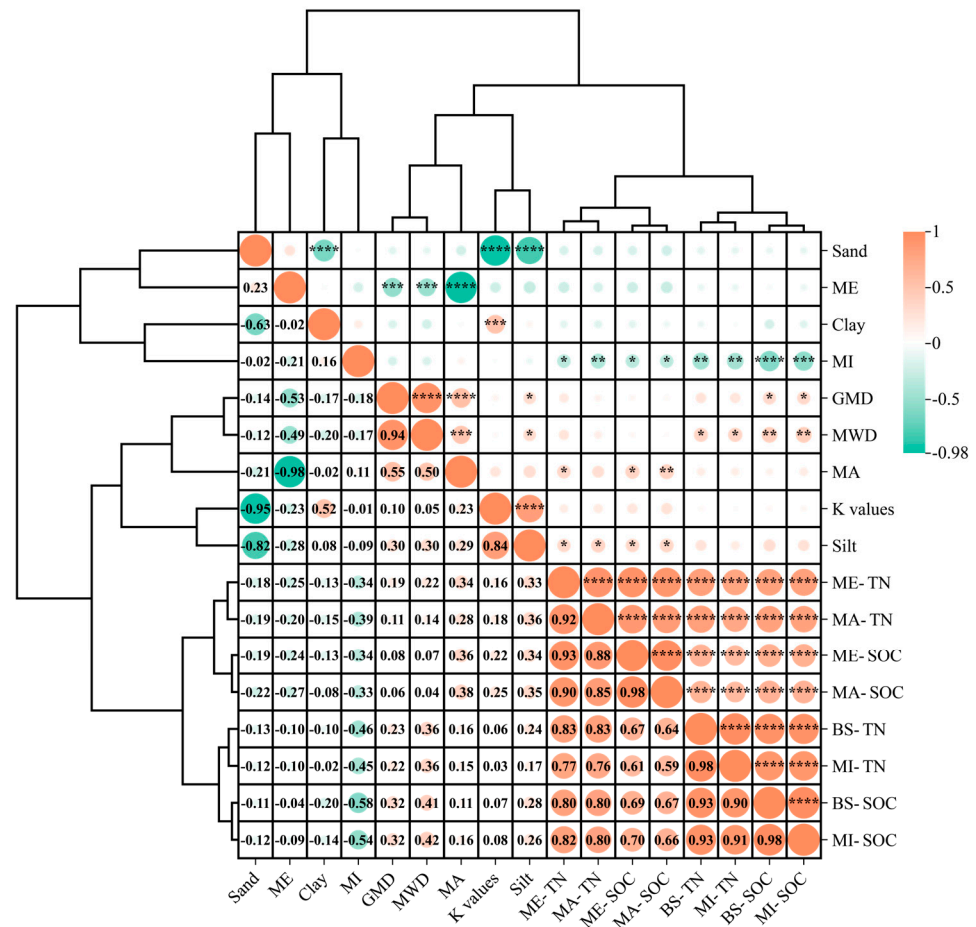

Figure 10. Correlation of relevant soil properties in different soil aggregates and whole soil. * is $p < 0.05$, ** is $p < 0.01$, *** is $p < 0.001$, and **** is $p < 0.0001$. BS-SOC, SOC content in whole soil; MA-SOC, macroaggregate-associated carbon content; ME-SOC, medium aggregate-associated carbon content; MI-SOC, microaggregate-associated carbon content; BS-TN, TN content in whole soil; MA-TN, macroaggregate TN content; ME-TN, mesoaggregate TN content; MI-TN, microaggregate TN content; MA, microaggregate content; ME, mesoaggregate content; MI, microaggregate content.

Land use type had a considerable impact on soil aggregate stability, according to the results of the partial least squares path model (PLS-PM). This effect was also indirectly influenced by environmental factors such as carbon and nitrogen pools, soil mechanical composition, and aggregate dispersion (Figure 11). Among these, the soil aggregate stability index had a significant negative correlation ($p < 0.05$) with soil mechanical composition (direct effect coefficient −0.931) and a significant positive correlation ($p < 0.05$) with land use type (direct effect coefficient 2.536) and carbon and nitrogen pools (direct effect coefficient 0.675). Furthermore, through impacting aggregate composition, soil mechanical composition indirectly impacted the amount of carbon and nitrogen in the pool (throughput coefficient 0.821).
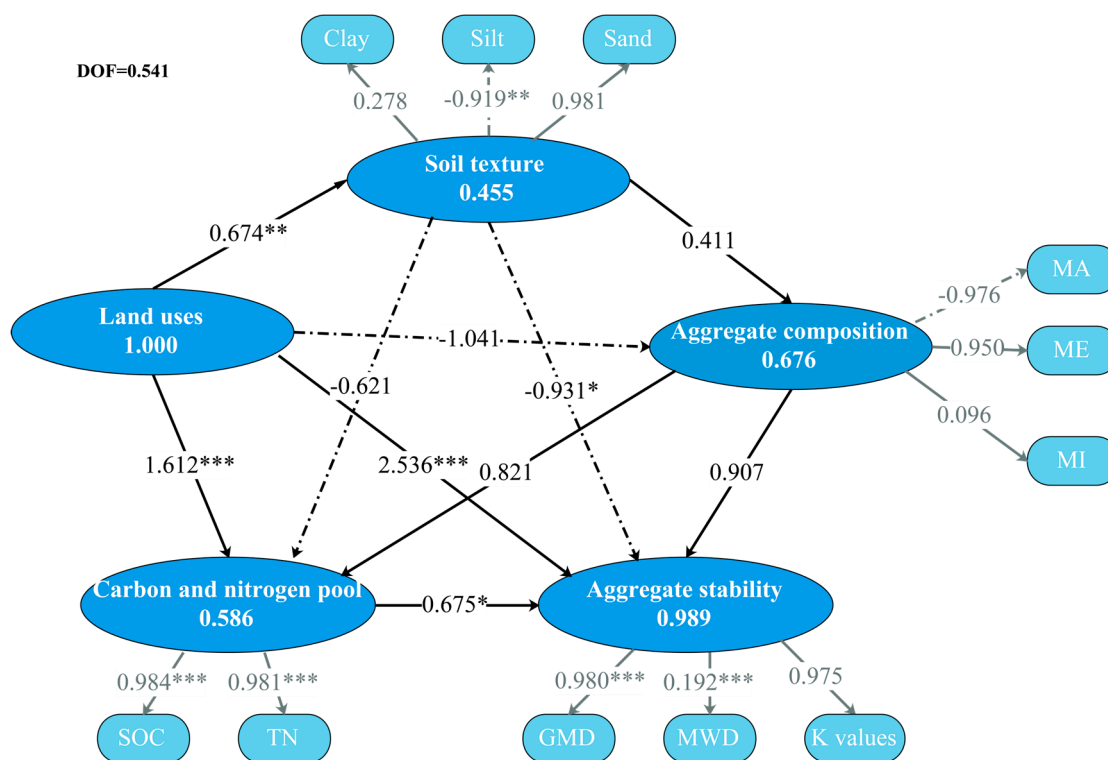
Figure 11. Causes of soil aggregate stability using the partial least squares path model (PL-SPM). The PL-SPM illustrates the connection between aggregate stability, carbon and nitrogen pools, soil characteristics, and land use practices. Gray lines show relationships between latent and display variables in the measurement model, whereas black lines show relationships between latent variables in the structural model. Path coefficients for positive or negative impacts are shown by values on solid lines and dashed arrows. * is $p < 0.05$, ** is $p < 0.01$, and *** is $p < 0.001$.

4. Discussion

4.1. Changes in Soil Aggregate Content and Stability Under Different Ecological Construction Measures

In this study, macroaggregates constituted the largest portion of soil aggregates, which is consistent with the findings of Yang et al. [30] in the southwest karst region. The number and distribution of macroaggregates reflect soil structural stability and resistance to erosion, contributing to plant growth and soil fertility improvement [10,40]. The Y1th–crt treatment significantly promoted the formation of medium and microaggregates, resulting in the highest proportion of these aggregate sizes among all treatments (Figure 3) and a more balanced distribution of aggregate proportions. This suggests that Y1th–crt has a higher potential to enhance macroaggregate formation. The likely reason for this is that the contour reverse-slope terrace measure reduces slope runoff by altering the microtopography, trapping runoff in "preferential entrainment" zones during rainfall. This runoff then infiltrates the soil, increasing soil porosity and improving permeability in the sloping cropland [41,42]. This, in turn, enhances the physical structure of the soil and facilitates the formation of medium and microaggregates. Medium soil particles contribute to water infiltration and aeration within the root zone due to their larger pore size, maintaining pore connectivity. These particles primarily bind with microaggregates through biological interactions, involving transient binders (such as microbial secretions, including polysaccharides and proteins) and short-term binders (such as roots and mycelium), which combine to form macroaggregates [1,43]. One previous study examining the effects of contour reverse-slope terrace measures on soil structure in the Songhua Dam sub-watershed in Yunnan Province demonstrated that these measures significantly improved soil aggregate composition. The

promotion of macroaggregate formation by these measures was further confirmed through the development of a Minimum Data Set (MDS) [35] and improved soil resistance to erosion, as confirmed by the contour reverse-slope terrace with its minimum erodibility. Consistently, our data suggest that contour reverse-slope terraces are particularly effective at promoting the formation and stabilization of large aggregates in karst landscapes. The well-developed and complex root system of natural vegetation fixes the soil, decreases erosion, and increases the accumulation of mucilage and flour while also creating favorable conditions for their formation (root decomposition and apoplastic matter). This may be the reason for the high content of mucilage and flour in restored forest and plantation forest treatments, according to the research [10].

Y7th–rgl exhibited the highest GMD in the 0–30 cm soil layer, indicating a higher degree of soil structural stability and effectiveness in promoting the formation of large soil aggregates. These large aggregates are crucial for enhancing soil structure and reducing susceptibility to erosion [19,33,44]. This finding is consistent with previous studies comparing aggregate stability at different stages of vegetation succession in the southwest karst region [30]. In this study, the plantation forest treatment (Y6th–jgl) resulted in the highest proportion of >0.25 mm aggregates. These aggregates facilitated the incorporation of organic matter and enhanced root–soil interactions, further promoting the process of soil agglomeration and stabilizing larger soil particles [45], contributing to a more stable soil structure. Y6th–jgl was particularly effective in improving aggregate stability in the topsoil layer, likely due to specific management practices, such as the optimized selection of plant species (kiwi) and field management techniques, including tilling and the incorporation of organic fertilizers. These practices encourage aggregate formation and improve soil structural integrity [46,47], as confirmed by the lower erodibility of meridional forests (Figure 5). In contrast, Y38th–ck exhibited the poorest structural stability and erodibility, indicating a decline in the quality of the tilled soil and increased erosion in the sloped cropland due to continuous year-round tillage. Rainfall breaks down soil aggregates into smaller particles, clogging soil pores and forming surface crusts, which increases surface runoff [47,48]. Moreover, frequent tillage, temperature change, or fire disrupts aggregate formation and reduces the stability of larger aggregates [49,50]. To address this, reducing tillage activities during the rainy season—when increased soil moisture can loosen soil structure and exacerbate erosion—may help promote soil stability. Future research should focus on the long-term effects of plantation forests on soil health over different time scales, as well as their potential application in broader ecological restoration projects.

4.2. Changes in Organic Carbon and TN in Soil Aggregates Under Different Ecological Construction Measures

Our results showed that microaggregates had the highest organic carbon and TN content across the five ecological construction measures. This may be attributed to the internal structural hierarchy of microaggregates, which have a compact structure and smaller pore spaces that effectively encapsulate and protect organic matter. This reduces the likelihood of microbial degradation, helps retain water and nutrients, and provides a favorable environment for microbial activity. Microorganisms within these aggregates break down organic matter and immobilize key nutrient elements (such as carbon, nitrogen, phosphorus, and micronutrients), thereby increasing organic carbon and TN content [23,50–52]. This is confirmed by the highest percentage of powder particles in this study. Powder particles can form microaggregates by combining them with cementing substances. In the 0–30 cm soil layer, the Y7th–rgl treatment showed the highest average organic carbon content across macroaggregates, microaggregates, and bulk soils. This suggests that Y7th–rgl was the most effective in increasing organic carbon storage in aggregate fractions and bulk soils, likely due to its superior soil structural stability (MWD = 4.35, GMD = 3.10) and higher

large aggregate content (60.11%) (Figures 2 and 3). Greater aggregate stability implies that large aggregates are more resilient to erosion caused by rainfall [20,53]. Additionally, plantation forests, which possess functional traits such as large leaf area, leaf thickness, root length, and root surface area, play a crucial role in carbon and nitrogen sequestration at multiple levels, including both the atmosphere and the lithosphere. These traits are key drivers of SOC and nitrogen dynamics [54,55]. Y7th–rgl also demonstrated high SRs for organic carbon and TN (SR_{SOC} = 1.35, 1.74; SR_{TN} = 1.35, 1.66), which significantly improved long-term soil nutrient stabilization, consistent with the findings of Deng et al. [25]. As a result, the organic carbon-rich macroaggregates were more resistant to displacement by rainwater erosion, thereby increasing the organic carbon content. This relationship between macroaggregate-associated content and organic carbon pools supports these findings.

In contrast, the lowest organic carbon and TN contents observed under the Y38th–ck treatment indicate its relative inefficiency in promoting soil carbon and nitrogen accumulation. This may be attributed to the continuous year-round tillage, which significantly reduces inputs from vegetation and soil, enhances microbial decomposition of carbon and nitrogen elements [4,56], and fails to prevent the loss of organic matter caused by rainfall runoff [41]. It is unsurprising that the lowest organic carbon and SRs (SR_{SOC} = 1.08, 1.11, SR_{TN} = 1.14, 1.27) were found in Y38th–ck in this study. These findings suggest that continuous tillage on sloping cropland leads to soil degradation, negatively affecting ecosystem function, soil health, and productivity [57,58]. The TN content in Y6th–zr exhibited higher values across all three soil aggregate sizes and in bulk soils, suggesting that Y6th–zr may be more effective in enhancing nitrogen retention than the other treatments. This could be due to the restored forestation measures, which may have favored nitrogen fixation or reduced nitrogen loss through leaching or volatilization [59,60].

The regression coefficients between soil aggregate carbon content and bulk SOC content increased with aggregate size in the 0–30 cm soil layer, indicating that organic carbon accumulation was significantly higher in large aggregates compared to medium and microaggregates. Conversely, the associated nitrogen content showed the opposite trend, suggesting that microaggregates play a more critical role in ecosystem nitrogen fixation [32,61]. Furthermore, the SRs of both organic carbon and TN were highest in the Y7th–rgl treatment, with significant increases in both ratios. This suggests a higher potential for nutrient accumulation near the soil surface, which is essential for maintaining plant productivity and soil fertility [22,25,62,63]. The TN partitioning rates in Y7th–rgl exceeded those of the other ecological construction measures, indicating that this treatment may be the most effective in enhancing nitrogen partitioning and nutrient availability in the topsoil. In contrast, the larger increase in organic carbon SRs for Y38th–ck and the smaller increase for Y1th–crt suggest that Y38th–ck exhibited greater disparities in organic carbon distribution across soil horizons, failing to enhance root nutrient availability. On the other hand, the SRs of organic carbon and TN of Y1th–crt were 1.02 to 1.12 times higher than those of the control treatment (Figure 4). This indicates that the contour reverse-slope terrace measure, with its unique "preferential entrainment" function, has a significant effect on improving soil and water conservation as well as soil nutrient retention in sloping cultivated land. Terrace tillage can significantly reduce the amount of sediment generated by surface area, as well as intercepting sediment upstream [64–66]. The contour reverse-slope terrace step increases the potential for chemical and particulate fractionation by controlling the "preferential entrainment" of soil nutrients, which enhances the spatial heterogeneity of SOC and TN distributions [67].

These findings emphasize the effectiveness of Y1th–crt, Y7th–rgl, and Y6th–zr in enhancing SOC and nitrogen content, particularly through their positive effects on soil aggregation and nutrient stratification. Therefore, contour anticlinal steps, plantations, and

natural revegetation measures hold significant potential for improving soil fertility and sustainability in karst landscapes. The long-term effects of these measures on soil health and ecosystem services merit further investigation.

4.3. Contribution of Same-Size Aggregates to Organic Carbon Pools and TN Pools

Soil aggregates of different grain sizes constitute bulk soil, and the organic carbon content in bulk soil is derived from the carbon pools formed by the associated carbon content of these aggregates [29]. In this study, macroaggregates contributed the most to both organic carbon and TN pools across the different ecological construction measures, consistent with previous findings [3,20]. This is likely due to the fact that microaggregates combine to form macroaggregates, and the high organic carbon content in macroaggregates can be attributed to the incorporation of organic matter during this process [29]. Organic matter within microaggregates gels together, while roots and fungal hyphae help decompose organic matter within macroaggregates, further promoting their formation [3]. Additionally, Pearson correlation analyses showed that macroaggregate content was strongly proportional to its associated stability, and macroaggregates were significantly and positively correlated with their organic carbon and TN contents (Figure 8). This suggests that macroaggregates play a critical role as carbon and nitrogen sinks within ecosystems. Notably, in the Y6th–jgl treatment, the contribution of macroaggregates to the organic carbon and TN pools reached 207% and 205%, respectively, significantly higher than the other treatments. This outcome can be attributed to the long-term accumulation of organic fertilizers, root secretions, and exudates during orchard management, which facilitated the formation of macroaggregates and their ability to adsorb and protect carbon and nitrogen nutrients [20]. Among medium aggregates, planted forests and naturally restored vegetation contributed the most to organic carbon and TN pools, aligning with the findings of Liu et al. [68] on afforestation in subtropical karst regions. This can be attributed to the input of root exudates and other organic materials in planted forests and naturally restored vegetation, which regulate the distribution of carbon and nitrogen across different aggregate sizes [69,70]. The effect of this process becomes more pronounced with the extension of afforestation [68].

In addition, the contribution of microaggregates to the organic carbon pool was highest in the Y6th–zr treatment (67%). This may be attributed to the strengthened interactions between the plant–soil system during restored forestation, which increased organic matter inputs, enhanced microbial activity, improved soil structure, and promoted the stabilization of carbon storage. The formation and stabilization of soil microaggregates were significantly enhanced, thereby increasing their contribution to organic carbon [10,30,56].

Overall, the contribution of soil aggregates to both organic carbon and TN pools was highest in the restored forestation treatment, indicating that restored forestation exerts a stronger regulatory effect on ecosystem function in karst areas.

4.4. Examining the Variables Influencing Collective Stability

According to PLS-PM, land use patterns, aggregate composition, and carbon and nitrogen pools are the primary determinants of soil aggregate stability. This finding is in line with the findings of Luo et al.'s study [71]. The size distribution and pore structure of soil aggregates can be greatly impacted by frequent patterns of soil disturbance. This makes it easier for microbes to metabolize and transform protected organic matter, which in turn affects the chemical transformation process of soil microbial loads and the breakdown of colloidal substances like organic matter and polysaccharides. Ultimately, these changes can impact the formation and stability of soil aggregates [72–74]. However, this study's aggregate composition effect throughput coefficient was not significant, suggesting that aggregate composition has a limited impact on soil aggregate stability. Consequently,

increasing the fraction of soil macroaggregates and stabilizing them necessitates raising the soil's carbon and nitrogen content. This enhances the soil aggregates' capacity to sequester carbon and hold onto nitrogen. Thus, anthropogenic disturbance and soil nutrient self-cycling combine to produce the structural stability of soil aggregates.

5. Conclusions

This study demonstrated the significant effects of different ecological construction measures on soil aggregate content and stability, as well as the changes in carbon and nitrogen contents within aggregates in karst landscapes. Among the various aggregate sizes, large aggregates had the highest content, highlighting their key role in promoting soil structure stability and supporting ecosystem function. In contrast, microaggregates were the main contributors to the soil carbon and nitrogen pools in the study area. Compared to other measures, the contour reverse-slope terrace measure significantly enhanced the formation of medium and microaggregates. This indicates that contour reverse-slope terraces provide the necessary substances for the formation and stabilization of macroaggregates, thereby increasing their formation potential. In comparison with traditional sloping cultivated land, the contour reverse-slope terrace measure promotes the spatial heterogeneity of organic carbon and TN through its unique "preferential entrainment" mechanism, maximizing the effectiveness of soil and water conservation over time. Planted forests exhibited high soil structure stability, playing a crucial role in improving the structure of karst soils. Notably, restored forestation measures contributed the most to carbon and nitrogen pools among all the ecological measures in this study, highlighting their superior ability to improve ecosystem functioning in fragile karst areas, which are characterized by weak soils, high erosion risk, and the need for advanced agricultural technology. The findings of this study enhance our understanding of the carbon and nitrogen sink functions, as well as the soil and water conservation aspects of different ecological construction measures in the karst region of southwest China.

References

1. Wang, F. Variations in Soil Aggregate Distribution and Associated Organic Carbon and Nitrogen Fractions in Long-Term Continuous Vegetable Rotation Soil by Nitrogen Fertilization and Plastic Film Mulching. *Sci. Total Environ.* **2022**, *835*, 155420. [CrossRef] [PubMed]
2. Dekemati, I.; Simon, B.; Vinogradov, S.; Birkás, M. The Effects of Various Tillage Treatments on Soil Physical Properties, Earthworm Abundance and Crop Yield in Hungary. *Soil Tillage Res.* **2019**, *194*, 104334. [CrossRef]
3. Mustafa, A. Soil Aggregation and Soil Aggregate Stability Regulate Organic Carbon and Nitrogen Storage in a Red Soil of Southern China. *J. Environ. Manag.* **2020**, *270*, 110894. [CrossRef] [PubMed]

4.	Dheri, G.S.; Lal, R.; Moonilall, N.I. Soil Carbon Stocks and Water Stable Aggregates under Annual and Perennial Biofuel Crops in Central Ohio. *Agric. Ecosyst. Environ.* **2022**, *324*, 107715. [CrossRef]

5.	Gan, F.; Shi, H.; Gou, J.; Zhang, L.; Dai, Q.; Yan, Y. Responses of Soil Aggregate Stability and Soil Erosion Resistance to Different Bedrock Strata Dip and Land Use Types in the Karst Trough Valley of Southwest China. *Int. Soil Water Conserv. Res.* **2023**, *12*, 684–696. [CrossRef]

6.	Breg Valjavec, M.; Čarni, A.; Žlindra, D.; Zorn, M.; Marinšek, A. Soil Organic Carbon Stock Capacity in Karst Dolines under Different Land Uses. *Catena* **2022**, *218*, 106548. [CrossRef]

7.	Yuan, J.; Liang, Y.; Zhuo, M.; Sadiq, M.; Liu, L.; Wu, J.; Xu, G.; Liu, S.; Li, G.; Yan, L. Soil Nitrogen and Carbon Storages and Carbon Pool Management Index under Sustainable Conservation Tillage Strategy. *Front. Ecol. Evol.* **2023**, *10*, 1082624. [CrossRef]

8.	Zhang, Y.; Xu, X.; Li, Z.; Liu, M.; Xu, C.; Zhang, R.; Luo, W. Effects of Vegetation Restoration on Soil Quality in Degraded Karst Landscapes of Southwest China. *Sci. Total Environ.* **2019**, *650*, 2657–2665. [CrossRef]

9.	Deng, L.; Kim, D.-G.; Peng, C.; Shangguan, Z. Controls of Soil and Aggregate–Associated Organic Carbon Variations Following Restored forest on the Loess Plateau in China. *Land Degrad. Dev.* **2018**, *29*, 3974–3984. [CrossRef]

10.	Dou, Y.; Yang, Y.; An, S.; Zhu, Z. Effects of Different Vegetation Restoration Measures on Soil Aggregate Stability and Erodibility on the Loess Plateau, China. *Catena* **2020**, *185*, 104294. [CrossRef]

11.	Nouwakpo, S.K.; Weltz, M.A.; Green, C.H.M.; Arslan, A. Combining 3D Data and Traditional Soil Erosion Assessment Techniques to Study the Effect of a Vegetation Cover Gradient on Hillslope Runoff and Soil Erosion in a Semi-Arid Catchment. *Catena* **2018**, *170*, 129–140. [CrossRef]

12.	Yue, L.; Juying, J.; Bingzhe, T.; Binting, C.; Hang, L. Response of Runoff and Soil Erosion to Erosive Rainstorm Events and Vegetation Restoration on Abandoned Slope Farmland in the Loess Plateau Region, China. *J. Hydrol.* **2020**, *584*, 124694. [CrossRef]

13.	Zhao, B.; Zhang, L.; Xia, Z.; Xu, W.; Xia, L.; Liang, Y.; Xia, D. Effects of Rainfall Intensity and Vegetation Cover on Erosion Characteristics of a Soil Containing Rock Fragments Slope. *Adv. Civ. Eng.* **2019**, *2019*, 7043428. [CrossRef]

14.	Lu, Y.; Dai, Q.; Yi, X.; Li, H.; Peng, H.; Tan, J. Impacts of Abandoned Sloping Farmland on Soil Aggregates and Aggregate– Associated Organic Carbon in Karst Rocky Desertification Areas. *Environ. Monit. Assess.* **2023**, *195*, 1404. [CrossRef] [PubMed]

15.	Tang, F.K.; Cui, M.; Lu, Q.; Liu, Y.G.; Guo, H.Y.; Zhou, J.X. Effects of Vegetation Restoration on the Aggregate Stability and Distribution of Aggregate–Associated Organic Carbon in a Typical Karst Gorge Region. *Solid Earth* **2016**, *7*, 141–151. [CrossRef]

16.	Zhu, D.; Yang, Q.; Zhao, Y.; Cao, Z.; Han, Y.; Li, R.; Ni, J.; Wu, Z. Afforestation Influences Soil Aggregate Stability by Regulating Aggregate Transformation in Karst Rocky Desertification Areas. *Forests* **2023**, *14*, 1356. [CrossRef]

17.	Zhang, Z.; Huang, X.; Zhou, Y. Spatial Heterogeneity of Soil Organic Carbon in a Karst Region under Different Land Use Patterns. *Ecosphere* **2020**, *11*, e03077. [CrossRef]

18.	Hoffland, E.; Kuyper, T.W.; Comans, R.N.J.; Creamer, R.E. Eco-Functionality of Organic Matter in Soils. *Plant Soil* **2020**, *455*, 1–22. [CrossRef]

19.	Anderson, R.; Brye, K.R.; Wood, L.S. Soil Aggregate Stability as Affected by Landuse and Soil Properties in the Lower Mississippi River Valley. *Soil Sci. Soc. Am. J.* **2019**, *83*, 1512–1524. [CrossRef]

20.	Cao, S.; Zhou, Y.; Zhou, Y.; Zhou, X.; Zhou, W. Soil Organic Carbon and Soil Aggregate Stability Associated with Aggregate Fractions in a Chronosequence of Citrus Orchards Plantations. *J. Environ. Manag.* **2021**, *293*, 112847. [CrossRef]

21.	Liu, C.; Wu, Z.; He, C.; Huang, B.; Zhang, Y.; Li, P.; Huang, W. Effect of Land Use Conversion on the Soil Aggregate–Associated Microbial Necromass Carbon in Estuarine Wetland of the Pearl River in China. *Catena* **2024**, *236*, 107761. [CrossRef]

22.	Liu, S.; Wang, R.; Yang, Y.; Shi, W.; Jiang, K.; Jia, L.; Zhang, F.; Liu, X.; Ma, L.; Li, C.; et al. Changes in Soil Aggregate Stability and Aggregate–Associated Carbon under Different Slope Positions in a Karst Region of Southwest China. *Sci. Total Environ.* **2024**, *928*, 172534. [CrossRef]

23.	Schweizer, S.A. Soil Microaggregate Size Composition and Organic Matter Distribution as Affected by Clay Content. *Geoderma* **2019**, *355*, 113901. [CrossRef]

24.	Totsche, K.U.; Amelung, W.; Gerzabek, M.H.; Guggenberger, G.; Klumpp, E.; Knief, C.; Lehndorff, E.; Mikutta, R.; Peth, S.; Prechtel, A.; et al. Microaggregates in Soils. *J. Plant Nutr. Soil Sci.* **2018**, *181*, 104–136. [CrossRef]

25.	Deng, J.; Sun, P.; Zhao, F.; Han, X.; Yang, G.; Feng, Y.; Ren, G. Soil C, N, P and Its Stratification Ratio Affected by Artificial Vegetation in Subsoil, Loess Plateau China. *PLoS ONE* **2016**, *11*, e0151446. [CrossRef] [PubMed]

26.	Zhang, W.; Munkholm, L.J.; Liu, X.; An, T.; Xu, Y.; Ge, Z.; Xie, N.; Li, A.; Dong, Y.; Peng, C.; et al. Soil Aggregate Microstructure and Microbial Community Structure Mediate Soil Organic Carbon Accumulation: Evidence from One-Year Field Experiment. *Geoderma* **2023**, *430*, 116324. [CrossRef]

27.	Lützow, M. Stabilization of organic matter in temperate soils: Mechanisms and their relevance under different soil conditions—A review. *Eur. J. Soil Sci.* **2006**, *57*, 426–445. [CrossRef]

28.	Paye, W.S.; Thapa, V.R.; Ghimire, R. Limited Impacts of Occasional Tillage on Dry Aggregate Size Distribution and Soil Carbon and Nitrogen Fractions in Semi-Arid Drylands. *Int. Soil Water Conserv. Res.* **2024**, *12*, 96–106. [CrossRef]

29.   Okolo, C.C.; Gebresamuel, G.; Zenebe, A.; Haile, M.; Eze, P.N. Accumulation of Organic Carbon in Various Soil Aggregate Sizes under Different Land Use Systems in a Semi-Arid Environment. *Agric. Ecosyst. Environ.* **2020**, *297*, 106924. [CrossRef]

30.   Yang, Y.; Wei, H.; Lin, L.; Deng, Y.; Duan, X. Effect of Vegetation Restoration on Soil Humus and Aggregate Stability within the Karst Region of Southwest China. *Forests* **2024**, *15*, 292. [CrossRef]

31.   Bai, X.; Ran, C.; Chen, J.; Luo, G.; Chen, F.; Xiao, B.; Long, M.; Li, Z.; Zhang, X.; Shen, X.; et al. Methods, progress and prospect for diagnosis of karst ecosystem health in China—An overview. *Chin. Sci. Bull.* **2023**, *68*, 2550–2568. [CrossRef]

32.   Bi, M.; Zhang, S.; Xu, Q.; Hou, S.; Han, M.; Yu, X. Coupling and Synergistic Relationships between Soil Aggregate Stability and Nutrient Stoichiometric Characteristics under Different Microtopographies on Karst Rocky Desertification Slopes. *Catena* **2024**, *243*, 108142. [CrossRef]

33.   Lan, J. Changes of Soil Aggregate Stability and Erodibility After Cropland Conversion in Degraded Karst Region. *J. Soil Sci. Plant Nutr.* **2021**, *21*, 3333–3345. [CrossRef]

34.   D'Ettorre, U.S.; Liso, I.S.; Parise, M. Desertification in Karst Areas: A Review. *Earth-Sci. Rev.* **2024**, *253*, 104786. [CrossRef]

35.   Li, M.; Wang, K.; Ma, X.; Fan, M.; Song, Y. Effects of Land Use Change on Soil Aggregate Stability and Erodibility in the Karst Region of Southwest China. *Agronomy* **2024**, *14*, 1534. [CrossRef]

36.   Ma, L.; Si, H.; Li, M.; Li, C.; Zhu, D.; Mao, Z.; Yan, Y.; Jiang, K.; Yu, P. Influence of Land Use Types on Soil Properties and Soil Quality in Karst Regions of Southwest China. *Agronomy* **2024**, *14*, 882. [CrossRef]

37.   Xu, Q.; Hou, L.; Wang, L.; Li, Q.; Wang, K. Contribution of glomalin-related soil protein to soil carbon and nitrogen storage in sloping farmland under contour reverse-slop terrace measures. *Acta Ecol. Sin.* **2023**, *44*, 2919–2930. [CrossRef]

38.   Chen, X.; Song, Y.; Wang, Z. Effect of contour reverse-slope terrace measures on soil water storage in sloping farmland of red soil in Central Yunnan Province. *Res. Soil Water Conserv.* **2019**, *26*, 92–99.

39.   Zhang, K.; Shu, A.; Xu, X.; Yang, Q.; Yu, B. Soil erodibility and its estimation for agricultural soils in China. *J. Arid Environ.* **2008**, *72*, 1002–1011. [CrossRef]

40.   Xiao, Y.; Ma, Z.; Jiang, Y.; Deng, Y. A Study on Soil Aggregate Stability and Splash Erosion under Exogenous Electrolyte Conditions in the Karst Region of Southwest China. *J. Hydrol. Reg. Stud.* **2024**, *53*, 101817. [CrossRef]

41.   Liang, Z.; Chen, X.; Wang, C.; Zhang, Z. Response of Soil Moisture to Four Rainfall Regimes and Tillage Measures under Natural Rainfall in Red Soil Region, Southern China. *Water* **2024**, *16*, 1331. [CrossRef]

42.   Wang, S.; Wang, K.; Song, Y.; Chen, X.; Wang, Z. Effects of contour reverse-slope terrace on nitrogen and phosphorus loss in sloping farmland in the water resource of area of Songhua Dam in Kunming City. *J. Soil Water Conserv.* **2017**, *31*, 7. [CrossRef]

43.   Rillig, M.C. Soil Aggregates as Massively Concurrent Evolutionary Incubators. *ISME J.* **2017**, *11*, 1943–1948. [CrossRef] [PubMed]

44.   Feng, H.; Wang, S.; Gao, Z.; Pan, H.; Zhuge, Y.; Ren, X.; Hu, S.; Li, C. Aggregate Stability and Organic Carbon Stock under Different Land Uses Integrally Regulated by Binding Agents and Chemical Properties in Saline-sodic Soils. *Land Degrad. Dev.* **2021**, *32*, 4151–4161. [CrossRef]

45.   Liu, Y.; Wang, P.; Wang, J. Formation and Stability Mechanism of Soil Aggregates: Progress and Prospect. *Acta Pedol. Sin.* **2023**, *60*, 627–643. [CrossRef]

46.   Yuan, J. Long-Term Organic Fertilization Enhances Potassium Uptake and Yield of Sweet Potato by Expanding Soil Aggregates-Associated Potassium Stocks. *Agric. Ecosyst. Environ.* **2023**, *358*, 108701. [CrossRef]

47.   Zhang, Z. Effect of Long-Term Combined Application of Organic and Inorganic Fertilizers on Soil Nematode Communities within Aggregates. *Sci. Rep.* **2016**, *6*, 31118. [CrossRef]

48.   Shi, P. Soil Aggregate Stability and Size-Selective Sediment Transport with Surface Runoff as Affected by Organic Residue Amendment. *Sci. Total Environ.* **2017**, *607*, 95–102. [CrossRef]

49.   Tobiašová, E.; Lemanowicz, J.; Dębska, B.; Kunkelová, M.; Sakáč, J. The Effect of Reduced and Conventional Tillage Systems on Soil Aggregates and Organic Carbon Parameters of Different Soil Types. *Agriculture* **2023**, *13*, 818. [CrossRef]

50.   Arunrat, N.; Kongsurakan, P.; Solomon, L.W.; Sereenonchai, S. Fire Impacts on Soil Properties and Implications for Sustainability in Rotational Shifting Cultivation: A Review. *Agriculture* **2024**, *14*, 1660. [CrossRef]

51.   Hartmann, M.; Six, J. Soil Structure and Microbiome Functions in Agroecosystems. *Nat. Rev. Earth Environ.* **2022**, *4*, 4–18. [CrossRef]

52.   Lehmann, J.; Kleber, M. The Contentious Nature of Soil Organic Matter. *Nature* **2015**, *528*, 60–68. [CrossRef]

53.   Dong, L.; Li, J.; Zhang, Y.; Bing, M.; Liu, Y.; Wu, J.; Hai, X.; Li, A.; Wang, K.; Wu, P.; et al. Effects of Vegetation Restoration Types on Soil Nutrients and Soil Erodibility Regulated by Slope Positions on the Loess Plateau. *J. Environ. Manag.* **2022**, *302*, 113985. [CrossRef] [PubMed]

54.   Dijkstra, F.A.; Zhu, B.; Cheng, W. Root Effects on Soil Organic Carbon: A Double-edged Sword. *New Phytol.* **2020**, *230*, 60–65. [CrossRef] [PubMed]

55.   Hu, W.; Lu, Z.; Meng, F.; Li, X.; Cong, R.; Ren, T.; Sharkey, D.; Lu, J. The Reduction in Leaf Area Precedes That in Photosynthesis under Potassium Deficiency: The Importance of Leaf Anatomy. *New Phytol.* **2020**, *227*, 1749–1763. [CrossRef]

56.	Yu, P.; Liu, J.; Tang, H.; Ci, E.; Tang, X.; Liu, S.; Ding, Z.; Ma, M. The Increased Soil Aggregate Stability and Aggregate–Associated Carbon by Farmland Use Change in a Karst Region of Southwest China. *Catena* **2023**, *231*, 107284. [CrossRef]

57.	Guo, S.; Zhai, L.; Liu, J.; Liu, H.; Chen, A.; Wang, H.; Wu, S.; Lei, Q. Cross-Ridge Tillage Decreases Nitrogen and Phosphorus Losses from Sloping Farmlands in Southern Hilly Regions of China. *Soil Tillage Res.* **2019**, *191*, 48–56. [CrossRef]

58.	Xin, X.; Sun, Z.; Xiao, J.; Feng, L.; Yang, N.; Liu, Y. Ridge-furrow Rainfall Harvesting Planting and Its Effect on Soil Erosion and Soil Quality in Sloping Farmland. *Agron. J.* **2021**, *113*, 863–877. [CrossRef]

59.	Sun, M.; Xiao, D.; Zhang, W.; Wang, K. Impacts of Managed Vegetation Restoration on Arbuscular Mycorrhizal Fungi and Diazotrophs in Karst Ecosystems. *J. Fungi* **2024**, *10*, 280. [CrossRef]

60.	Xiao, Z. Nitrogen and Phosphorus Change the Early Restored forest in Degraded Phaeozems of Gullies. *Sci. Total Environ.* **2023**, *888*, 164107. [CrossRef]

61.	Zhao, G.; Cong, M.; Zhang, Z.; Zeng, F.; Dong, X.; Song, J. Microaggregates Regulate the Soil Organic Carbon Sequestration and Carbon Flow of Windproof Sand Fixation Forests in Desert Ecosystems. *Catena* **2024**, *245*, 108320. [CrossRef]

62.	Ferreira, C.D.R.; Silva Neto, E.C.D.; Pereira, M.G.; Guedes, J.D.N.; Rosset, J.S.; Anjos, L.H.C.D. Dynamics of Soil Aggregation and Organic Carbon Fractions over 23 Years of No-till Management. *Soil Tillage Res.* **2020**, *198*, 104533. [CrossRef]

63.	Yu, P.; Tang, X.; Liu, S.; Liu, W.; Zhang, A. Short Term Effects of Revegetation on Labile Carbon and Available Nutrients of Sodic Soils in Northeast China. *Land* **2020**, *9*, 10. [CrossRef]

64.	Londero, A.L. Impact of Broad-Based Terraces on Water and Sediment Losses in No-till (Paired Zero-Order) Catchments in Southern Brazil. *J. Soils Sediments* **2017**, *18*, 1159–1175. [CrossRef]

65.	Meng, X.; Zhu, Y.; Shi, R.; Yin, M.; Liu, D. Rainfall–Runoff Process and Sediment Yield in Response to Different Types of Terraces and Their Characteristics: A Case Study of Runoff Plots in Zhangjiachong Watershed, China. *Land Degrad. Dev.* **2023**, *35*, 1449–1465. [CrossRef]

66.	Bai, J.; Yang, S.; Zhang, Y.; Liu, X.; Guan, Y. Assessing the Impact of Terraces and Vegetation on Runoff and Sediment Routing Using the Time-Area Method in the Chinese Loess Plateau. *Water* **2019**, *11*, 803. [CrossRef]

67.	Hou, T. Tillage-Induced Surface Soil Roughness Controls the Chemistry and Physics of Eroded Particles at Early Erosion Stage. *Soil Tillage Res.* **2020**, *207*, 104807. [CrossRef]

68.	Liu, L.; Zhu, Q.; Wan, Y.; Yang, R.; Mou, J.; Li, Y.; Meng, L.; Zhu, T.; Elrys, A.S. Afforestation Improves Soil Organic Carbon and Total Nitrogen Stocks Mainly through Increasing > 2 Mm Aggregate Fractions and Stimulating Carbon and Nitrogen Transformations within Aggregates in Subtropical Karst Region. *Catena* **2024**, *243*, 108220. [CrossRef]

69.	Bhattacharyya, R. Soil Organic Carbon Is Significantly Associated with the Pore Geometry, Microbial Diversity and Enzyme Activity of the Macro-Aggregates under Different Land Uses. *Sci. Total Environ.* **2021**, *778*, 146286. [CrossRef]

70.	Stainsby, A.; May, W.E.; Lafond, G.P.; Entz, M.H. Soil Aggregate Stability Increased with a Self-Regenerating Legume Cover Crop in Low-Nitrogen, No-till Agroecosystems of Saskatchewan, Canada. *Can. J. Soil. Sci.* **2019**, *100*, 314–318. [CrossRef]

71.	Luo, T.; Xia, L.; Xia, D.; Liu, W.; Xu, Y.; He, Z.; Xu, W. Impact of Typical Land Use Type on the Stability and Content of Carbon and Nitrogen of Soil Aggregates in Western Hubei. *Ecosphere* **2023**, *14*, e4736. [CrossRef]

72.	Luo, L.; Meng, H.; Wu, R.; Gu, J.-D. Impact of Nitrogen Pollution/Deposition on Extracellular Enzyme Activity, Microbial Abundance and Carbon Storage in Coastal Mangrove Sediment. *Chemosphere* **2017**, *177*, 275–283. [CrossRef] [PubMed]

73.	Wang, Y.; Ran, L.; Fang, N.; Shi, Z. Aggregate Stability and Associated Organic Carbon and Nitrogen as Affected by Soil Erosion and Vegetation Rehabilitation on the Loess Plateau. *Catena* **2018**, *167*, 257–265. [CrossRef]

74.	Zhang, Y. Effects of Farmland Conversion on the Stoichiometry of Carbon, Nitrogen, and Phosphorus in Soil Aggregates on the Loess Plateau of China. *Geoderma* **2019**, *351*, 188–196. [CrossRef]